doi: 10.18323/2782-4039-2025-3-73-1

Features of arc surfacing of intermetallic alloys of the Fe–Al system on the surface of low-carbon steels

Aleksandr G. Bochkarev*[1,3], PhD (Engineering),
assistant professor of Chair "Welding, Pressure Material Treatment and Related Processes"
Aleksandr I. Kovtunov[1,4], Doctor of Sciences (Engineering),
professor of Chair "Welding, Pressure Material Treatment and Related Processes"
Denis I. Plakhotny[1,5], senior lecturer
of Chair "Welding, Pressure Material Treatment and Related Processes"
Yuri Yu. Khokhlov[1,6], Head of the Laboratory
of Chair "Welding, Pressure Material Treatment and Related Processes"
Savely O. Belonogov[2,7], engineer
of the Laboratory of Destructive Inspection Methods
Ivan V. Vedeneev[2,8], engineer
of the Laboratory of Non-Destructive Inspection

[1]*Togliatti State University, Togliatti (Russia)*
[2]*LLC Middle Volga Certification and Diagnostic Center "Delta", Togliatti (Russia)*

***E-mail:** a.bochkarev5@tltsu.ru,
a.bochkarev93@mail.ru

[3]ORCID: https://orcid.org/0000-0002-7945-1634
[4]ORCID: https://orcid.org/0000-0002-7705-7377
[5]ORCID: https://orcid.org/0000-0003-2021-8974
[6]ORCID: https://orcid.org/0000-0002-5276-8957
[7]ORCID: https://orcid.org/0009-0007-9788-9967
[8]ORCID: https://orcid.org/0009-0009-4159-526X

Received 17.04.2025 *Revised 10.06.2025* *Accepted 13.08.2025*

Abstract: The durability of industrial components is largely determined by the materials they are made of. Often, the materials used must be resistant to wear, corrosion, and high temperatures. Advanced materials, such as high-strength alloy steels, are expensive and have limited weldability, which complicates the restoration of worn components. Fe–Al alloys having high corrosion resistance, wear resistance, and heat resistance at a lower cost are considered as an alternative. The objective of this study is to increase the wear resistance and heat resistance of low-carbon steel components by studying the processes of arc surfacing of iron aluminides and their properties. The study methodology included single-arc and double-arc surfacing using aluminium and steel electrode wires, analysis of the chemical composition of the deposited coatings, their hardness, wear resistance, and heat resistance. The results showed that single-arc surfacing forms alloys based on $FeAl_3$ and α-Al phases with Fe_2Al_5 and $FeAl_3$ inclusions, while double-arc surfacing produces alloys more saturated with iron with an α-Fe matrix phase and a Fe_3AlC_x carbide phase. The resulting alloys demonstrate a hardness of up to 58 HRC, a relative wear resistance of up to 2.5 units, and a weight loss of no more than 5 % with an aluminium content of up to 20 %, which indicates their potential for use under high loading conditions. The results confirm the feasibility of using iron aluminides as an inexpensive alternative to expensive coatings, which expands the possibilities for increasing the wear resistance and heat resistance of components in industry.

Keywords: arc surfacing; intermetallic alloys; iron aluminides; low-carbon steel; hardness; wear resistance; heat resistance.

For citation: Bochkarev A.G., Kovtunov A.I., Plakhotny D.I., Khokhlov Yu.Yu., Belonogov S.O., Vedeneev I.V. Features of arc surfacing of intermetallic alloys of the Fe–Al system on the surface of low-carbon steels. *Frontier Materials & Technologies*, 2025, no. 3, pp. 11–25. DOI: 10.18323/2782-4039-2025-3-73-1.

INTRODUCTION

The productivity and competitiveness of mining enterprises largely depend on the reliability and wear resistance of the equipment in operation. The main problems faced by enterprises are related to the reduction of the service life of components, increased downtime due to wear and tear and breakdowns, as well as increased costs for repairs and spare parts. The problem of increasing the wear resistance of parts subject to abrasive and corrosive wear, which directly affects the technical and economic indicators of enterprises and the cost of products, is particularly relevant. Under conditions of intensive operational loads, the materials of the parts wear out quickly, which necessitates frequent repairs and replacement of equipment elements.

In recent decades, research has been actively conducted in the field of increasing the wear resistance of mining equipment. Thus, in works [1; 2] it is noted that about 50 % of equipment downtime is associated with the restoration of the surfaces of components damaged by abrasive wear. An important aspect is the use of materials with increased

corrosion and wear resistance. For example, high-strength medium-alloy steels (35HGSL, 38H2NMA, 20HGSN2MFA) are used for parts operating under high loads, but their cost is quite high. In this regard, in most cases, more affordable carbon and low-alloy steels are used (3, 20, 10HSND, 12H1M steels), which have good wear resistance and are easy to repair [3].

Particular attention is paid to the application of protective coatings, which can significantly increase the wear resistance and corrosion resistance of parts. The literature describes spraying and surfacing methods, such as plasma, arc and gas-flame spraying, as well as arc metallisation [4; 5]. However, despite the effectiveness of these methods, due to the limited thickness of the protective layers (from 10 to 200 μm) and their tendency to failure under loads, their use requires further research.

An interesting direction is the use of intermetallic alloys of the Fe–Al system [6; 7], which have high corrosion [8] and heat resistance [9], as well as the ability to form protective coatings up to several millimeters thick. In [10; 11], it is shown that such materials can significantly increase the wear resistance of parts. In [12], the mechanical properties of iron aluminides are shown when heated to 600 °C, in [13], the results of the study of intermetallic alloys of the Fe–Al system under high-temperature cyclic oxidation at temperatures of 800, 900 and 1000 °C are presented, which confirms the possibility of using these materials at elevated temperatures. In [14], the successful use of iron aluminides during operation at elevated temperatures (up to 950 °C) is shown. However, at present, the possibilities of their use for the restoration of mining equipment parts have not been sufficiently studied, which makes further research relevant.

Known methods of applying iron aluminides to the surface of steel parts are friction application of aluminium and iron powder [15] or application of aluminium powder only [16] followed by annealing of the part in a furnace. Other known methods of applying iron aluminides are self-propagating high-temperature synthesis [17], laser cladding [18], various spraying methods (plasma spraying, vacuum plasma spraying, gas-flame spraying) [14].

The presented methods of applying protective coatings based on iron aluminides allow obtaining coatings with a limited layer thickness of up to 0.5 mm, which is clearly insufficient for mining equipment components operating under abrasive wear conditions. Another significant limitation is the impossibility of applying the coating in installation conditions and the lack of prospects for further restoration of the coating after wear. Therefore, despite a significant amount of research, issues related to the optimisation of the technologies of protective coating application, their durability and resistance to mechanical and chemical influences remain unresolved. In particular, the processes of formation of intermetallic coatings on parts made of low-carbon steels, as well as their behaviour under operating conditions of mining equipment, have not been sufficiently studied. Moreover, there is a necessity of developing inexpensive and effective methods for restoring worn surfaces that can ensure a long service life of parts.

The aim of this study is to increase the wear resistance and heat resistance of parts made of low-carbon steel by studying the processes of arc surfacing of iron aluminides and their properties.

METHODS

The study of the processes of surfacing of Fe–Al intermetallic alloys was carried out by single-arc surfacing using an aluminium electrode wire (Fig. 1) and double-arc surfacing using steel and aluminium electrode wires (Fig. 2).

The authors used SvA7 solid electrode wire according to GOST 7871-2019 as surfacing material for single-arc surfacing and Sv-08G2S wire according to GOST 2246-70 and SvA7 wire according to GOST 7871-2019 for double-arc surfacing. The diameter of the wires used was 1.2 mm. High-grade argon according to GOST 10157-2016 was used as a gas shield. Surfacing was carried out on plates made of steel 20 according to GOST 1577-2022 with overall dimensions of 160×80 mm and a thickness of 10 mm. As the welding equipment, Megatronic BDH 550 (Denmark) was used.

The single-arc surfacing modes were varied in a wide range: arc voltage (*U*arc Al) – from 10 to 30 V; surfacing speed (*V*s) – from 0.1 to 0.2 m/min; speed of aluminium electrode wire feed (*V*f/w Al) – from 3 to 6 m/min; shielding gas flow rate – from 10 to 14 l/min. The torch tilt angle (α) during single-arc surfacing was varied from 90 to 30° with a step of 15°. The double-arc surfacing modes were varied in the following ranges: arc voltage when using aluminium electrode wire (*U*arc Al) – from 14 to 18 V; arc voltage when using Sv-08G2S electrode wire (*U*arc St) – from 23.5 to 27.5 V; surfacing speed (*V*s) – 0.1 to 0.2 m/min; speed of aluminium electrode wire feed (*V*f/w Al) – from 3 to 5 m/min; speed of Sv-08G2S electrode wire feed (*V*f/w St) – from 3 to 4 m/min; shielding gas flow rate – from 10 to 14 l/min. The angle of inclination of the torches (α) for double-arc surfacing was 55°.

The geometric parameters of the welding beads were determined on pre-etched samples (in a 20 % HNO_3 solution) cut in cross section (Fig. 3). The measurement was carried out using the Universal Desktop Ruler program by setting the scale factor and subsequent measurement of the width of the welding bead (*e*), the height of the welding bead reinforcement (*g*), and the depth of fusion penetration (*h*) (Fig. 3).

The influence of the electrode wire feed angle on the stability of the surfacing process and the geometric parameters of the deposited alloys, such as the width of the welding bead (*e*), the height of the welding bead reinforcement (*g*) and the depth of fusion penetration (*h*) were assessed by changing the torch tilt angle from 30 to 90° with a step of 15°.

The volume of intermetallic inclusions in the matrix alloy was assessed using microstructure images obtained with a microscope. Taking into account the scale factor, the volume of all inclusions in the image was measured and compared with the total volume of the matrix in the same image.

The chemical composition was analysed by scanning electron microscopy (SEM) using a LEO 1455 VP scanning

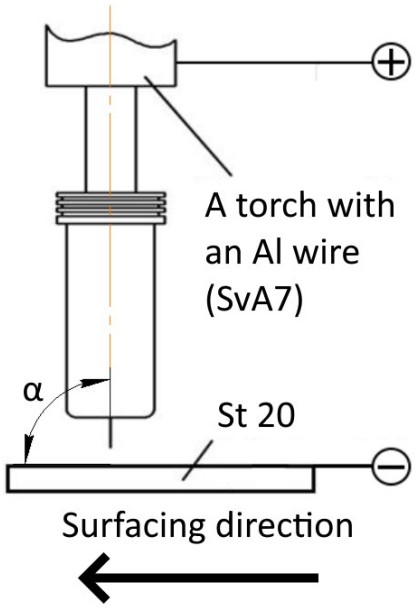

Fig. 1. *Scheme of single-arc surfacing of Fe–Al system intermetallic alloys with a consumable electrode in a shielding gas environment. α is wire feed angle*
Рис. 1. *Схема однодуговой наплавки плавящимся электродом в среде защитных газов интерметаллидных сплавов системы Fe–Al. α – угол ввода проволоки*

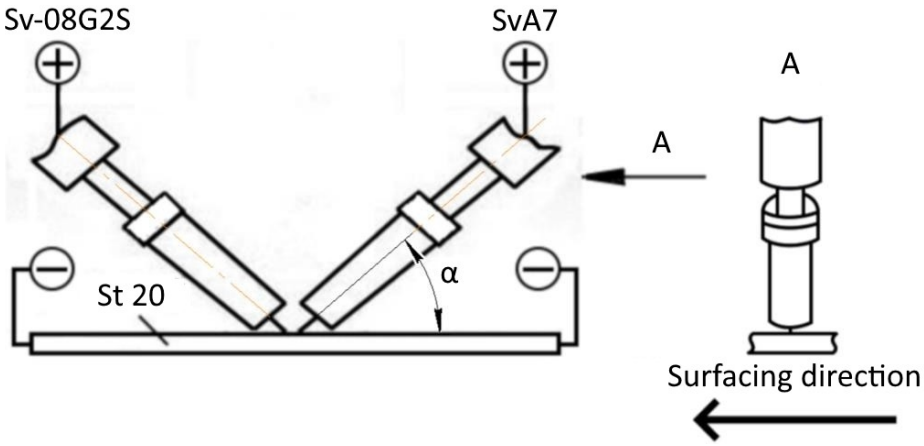

Fig. 2. *Scheme of double-arc surfacing with the feed of steel and aluminium electrode wires. α is wire feed angle*
Рис. 2. *Схема двухдуговой наплавки с подачей стальной и алюминиевой электродных проволок. α – угол ввода проволоки*

electron microscope (ZEISS, Germany) with INCA Energy-300 X-ray energy spectrometer (UK) and INCA Wave-500 X-ray wave spectrometer (UK) units and an HKL Premium EBSD System (UK) electron backscatter diffraction recording and analysis system. The samples for the studies were ground cross-sectional surfaces after surfacing Fe–Al beads onto grade 20 steel plates. Due to the insufficient quality of grinding for implementing the electron backscatter diffraction technique and reliably determining the elemental composition of the deposited metal in its various areas, chemical etching of the grinding surface was performed with a reagent of 3 ml HF + 3 ml HNO_3 + 94 ml H_2O. Fig. 4 shows a diagram of the selection of points for determining the chemical composition of the deposited metal.

X-ray diffraction analysis (XRD) was performed on a Bruker D8 Advance Eco X-ray diffractometer (Bruker AXS GmbH) (Germany) with a vertical θ-θ goniometer. For deposited samples with an uneven surface, it is preferable to use a parallel-beam geometry shooting scheme. To implement it, a Goebel mirror was installed on the primary beam using the linear focus of the X-ray tube. Goebel mirror is a multilayer heterostructure on a parabolically curved substrate that transforms the diverging beam into a parallel

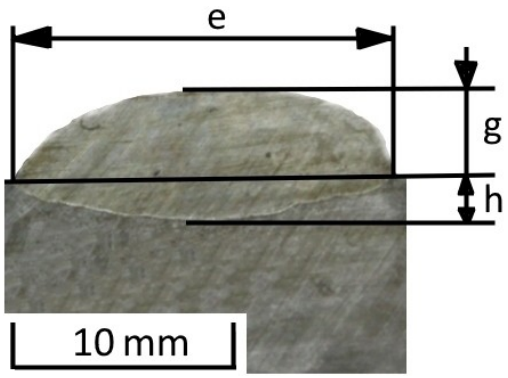

Fig. 3. *Cross-section of the deposited metal for measuring geometric parameters*
Рис. 3. *Поперечное сечение наплавленного металла для измерения геометрических параметров*

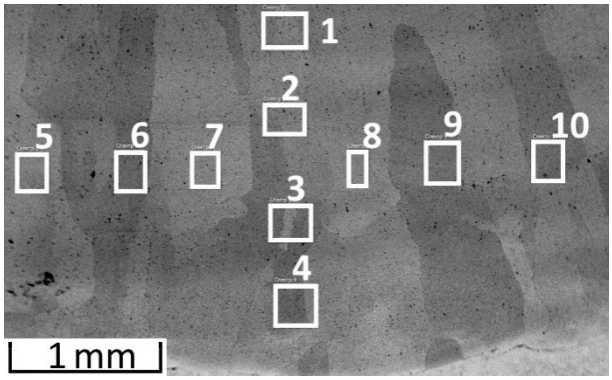

Fig. 4. *Scheme of selection of points for chemical composition study*
Рис. 4. *Схема выбора точек для исследования химического состава*

quasi-monochromatic one with a divergence angle of 0.03°. A collimator with a diameter of 1.0 mm was used to truncate the X-ray radiation “spot”. The shooting point was preliminarily cleaned with sandpaper. The samples under study were shot in copper anode radiation (λ=1.54060 Å). The tube voltage was 40 kV; the heating current was 25 mA. The exposure time was 1 s; the scanning step was 0.02°. Focusing on the test area and bringing the sample surface to the centre of the focusing circle were performed using a laser guidance system. The samples were examined for reflection; the intensity of the diffraction pattern was recorded using an SSD160 linear-type position-sensitive detector (Germany) with 160 channels. Phase identification was performed in the software for the Diffrac EVA diffractometer (version 4.2.1) (USA) using the licensed Powder Diffraction File-2 database (The International Center for Diffraction Data).

Rockwell hardness of the deposited alloys was measured according to GOST 9013-59. The measurements were carried out using the HRC scale on an ITBRV-187.5-A hardness tester.

The wear resistance of the deposited alloys was assessed by testing samples for friction against fixed abrasive particles according to GOST 17367-71. For a more accurate assessment of the relative wear resistance, the comparison of the test and reference samples was carried out by measuring the linear and weight wear according to the formula:

$$\varepsilon = \frac{\Delta l_s}{\Delta l_m},$$

where l_s is the wear of the standard;
Δl_m is the wear of the test material.

Steel 45 was used as the reference material to determine the degree of wear.

To study wear resistance, an installation that ensures a stable load on the test sample was used (Fig. 5). The installation consists of a frame with a fixed drive connected to a metal disk. The metal disk is equipped with clamps using which abrasive paper is attached to it. A vice for installing test samples is located on the frame under the disk. The installation is equipped with a timer that allows setting the required test time. The pressure on the sample during testing is regulated by installing weights on the lever.

Thermal resistance was determined by holding the samples in a SNOL 30/1100 muffle furnace at a temperature

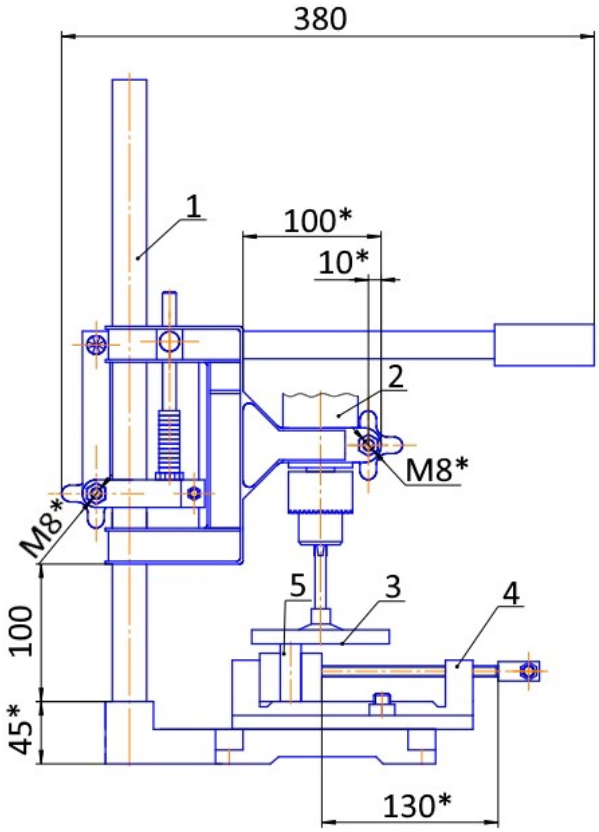

Fig. 5. *Installation for testing wear resistance of deposited samples:*
1 – frame; 2 – drive; 3 – metal disk with clamps; 4 – vice; 5 – test sample
Рис. 5. *Установка для испытания износостойкости наплавленных образцов:*
1 – станина; 2 – привод; 3 – металлический диск с зажимами; 4 – тиски; 5 – испытуемый образец

of 950 °C, then weighing them at equal intervals. Based on the data obtained, diagrams were compiled showing the dependence of the change in the mass of the samples on the time spent in the furnace at a certain temperature (950 °C).

RESULTS

Studies of single-arc surfacing of aluminium electrode wire on steel 20 have shown that in the selected range of modes, beads with different geometric parameters and stability of the surfacing process are formed. It is possible to conditionally divide the ranges of modes in which beads with low, medium and high stability of the surfacing process are formed. As a criterion for the stability of the surfacing process, the homogeneity of the geometric parameters of the surfacing beads in height and width was chosen. This criterion indicates the stability of droplet transfer during the formation of welding beads, and is necessary for surfacing and ensuring a more uniform distribution of chemical elements and the absence of defects in the form of inter-bead lack of fusion during multi-pass surfacing.

Low stability of the surfacing processes (Fig. 6) is observed in the following modes: feed rate of the aluminium electrode wire (*V*f/w Al) is 3 m/min with an arc voltage range (*U*arc Al) from 10 to 20 V. The surfacing speed (*V*s) in this case is from 0.1 to 0.2 m/min. With an increase in voltage indicators in the specified range of modes, fusion of the current-carrying tip of the torch is observed. With an increase in the feed rate of the aluminium electrode wire to 4 m/min, with all other parameters specified above being equal, medium stability of the surfacing process is observed (Fig. 7). In this range of modes, a more uniform formation of welding beads is observed.

Increasing the arc voltage (*U*arc Al) to 22.5 V at a feed rate of the aluminium electrode wire (*V*f/w Al) of 4 m/min in the surfacing speed range (*V*s) from 0.1 to 0.2 m/min leads to a decrease in the stability of the surfacing process (Fig. 8), and an arc voltage above 22.5 V leads to melting of the current-carrying tip.

At a feed rate of the aluminium electrode wire (*V*f/w Al) from 5 to 6 m/min with an arc voltage (*U*arc Al) from 15 to 25 V and a surfacing speed (*V*s) from 0.1 to 0.2 m/min, beads with stable geometric parameters are observed (Fig. 9).

The stability of the surfacing process is determined primarily by the surfacing modes, however, the stability of the surfacing process and the quality of the formation of the deposited alloys are also affected by the angle of the electrode wire feed relative to the surface being surfacing.

It is noted that by changing the torch tilt angle (α) from 30 to 90°, one can observe a slight decrease in the width (*e*)

Fig. 6. *External appearance of the welding bead produced in the following mode: Vf/w Al=3 m/min; Uarc Al=20 V; Vs=0.15 m/min*
Рис. 6. *Внешний вид наплавленного валика, полученного при следующем режиме: Vп/п Al=3 м/мин; Uд Al=20 В; Vн=0,15 м/мин*

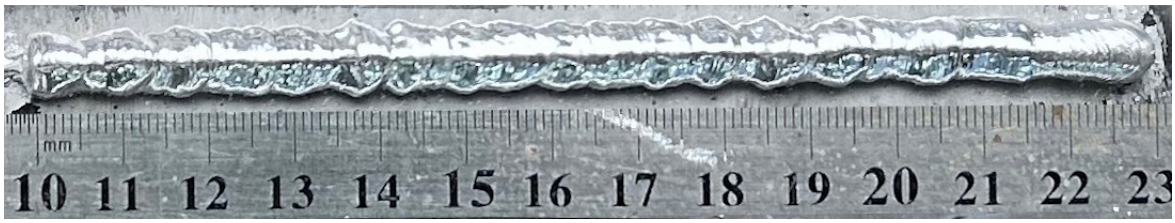

Fig. 7. *External appearance of the welding bead produced in the following mode: Vf/w Al=4 m/min; Uarc Al=12.5 V; Vs=0.15 m/min*
Рис. 7. *Внешний вид наплавленного валика, полученного при следующем режиме: Vп/п Al=4 м/мин; Uд Al=12,5 В; Vн=0,15 м/мин*

Fig. 8. *External appearance of the welding bead produced in the following mode: Vf/w Al=4 m/min; Uarc Al=22.5 V; Vs=0.1 m/min*
Рис. 8. *Внешний вид наплавленного валика, полученного при следующем режиме: Vп/п Al=4 м/мин; Uд Al=22,5 В; Vн=0,1 м/мин*

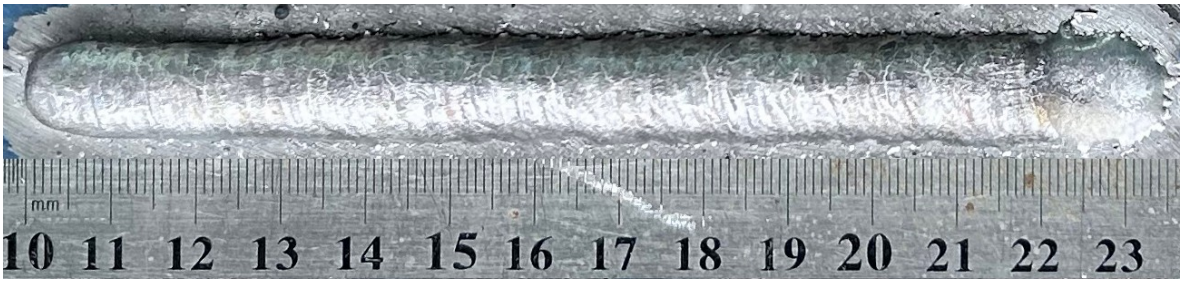

Fig. 9. *External appearance of the welding bead produced in the following mode: Vf/w Al=6 m/min; Uarc Al=25 V; Vs=0.15 m/min*
Рис. 9. *Внешний вид наплавленного валика, полученного при следующем режиме: Vп/п Al=6 м/мин; Uд Al=25 В; Vн=0,15 м/мин*

of the welding beads and a slight increase in the height of the welding beads (*g*) and the weld penetration depth (*h*). An increase in the torch tilt angle by 1° leads to a decrease in the weld width by approximately 0.038 mm, an increase in the weld height by 0.016 mm and an increase in the weld penetration depth by approximately 0.003 mm. To the greatest extent, a change in the torch tilt angle from 90 to 30° leads to an increase in the electrode wire losses due to spatter (Fig. 10).

The geometric parameters of the welding beads depend on the surfacing modes. An increase in the arc voltage (*U*arc Al) in the specified range of modes leads to an increase in the width of the welding beads (*e*) and an insignificant increase in the weld penetration depth (*h*), while the height of the welding beads (*g*) decreases. An increase in the surfacing speed (*V*s) in the specified range of modes leads to a decrease in the width (*e*) and height (*g*) of the welding beads, while the weld penetration depth (*h*) increases slightly. An increase in the rate of the aluminium electrode wire feed (*V*f/w Al) in the specified range of modes leads to an increase in the geometric parameters of the welding alloys, such as the width (*e*) and height (*g*) of the welding beads and the weld penetration depth (*h*) of the base metal. The geometric parameters of the deposited alloys in single-arc surfacing are described by regression equations:

$$e = -0.542 + 0.557 \times Uarc\,\mathrm{Al} - 22.437 \times Vs + \\ + 1.258 \times Vf/w\,\mathrm{Al} - 0.098 \times \alpha;$$

$$g = 7.309 - 0.136 \times Uarc\,\mathrm{Al} - 16.460 \times Vs + \\ + 0.281 \times Vf/w\,\mathrm{Al} + 0.016 \times \alpha;$$

$$h = -1.703 + 0.044 \times Uarc\mathrm{Al} + 0.476 \times V\mathrm{s} + \\ + 0.146 \times Vf/w\,\mathrm{Al} + 0.003 \times \alpha.$$

It was found that from the wide range of surfacing modes considered, intermetallic alloys of the Fe–Al system are formed in a narrower range of modes. Intermetallic alloys are formed under the following surfacing modes: rate of the aluminium electrode wire feed (*V*f/w Al) is 5–6 m/min; arc voltage (*U*arc Al) is 20–25 V; surfacing speed (*V*s) is 0.1–0.2 m/min. At an arc voltage above 25 V, melting of the current-carrying tip is observed, and at a voltage below 20 V, no weld penetration of the base metal is observed (Fig. 11), and the deposited alloy is pure aluminium, which is not suitable for use as a protective coating on steel parts. At a rate of the aluminium electrode wire feed less than 5 m/min in the entire range of modes, the deposited metal is an aluminium coating on steel.

The aluminium content in the welding intermetallic beads varies in the range from 71.49 to 94.21 wt. % at a torch tilt angle of 90° (angle of electrode wire feed relative to the product surface).

The aluminium content in the deposited metal depends on the surfacing modes. The rate of the aluminium electrode wire feed (*V*f/w Al) (Fig. 12) and the speed of surfacing (*V*s) (Fig. 13) exert the greatest influence. Arc voltage, all other parameters being equal, reduces the aluminium content in the deposited metal, but the effect of arc voltage (*U*arc Al) is statistically insignificant in its value and has virtually no effect on the chemical composition. With an increase in arc voltage by 1 V, all other parameters being equal, a decrease in the aluminium content in the deposited metal by 0.3 wt. % is observed.

The study of the chemical composition of iron aluminides and its structural components showed that the deposited metal is represented by a matrix alloy based on the $FeAl_3$+α-Al phases with inclusions of the Fe_2Al_5 and $FeAl_3$ intermetallic phases (Fig. 14). However, producing deposited alloys with the Fe_2Al_5 and $FeAl_3$ phases is undesirable due to high brittleness. As the research results showed, the deposited metal is destroyed (peels off from the substrate) along the fusion line, where the content of brittle intermetallic inclusions based on the Fe_2Al_5 and $FeAl_3$ phases is maximal (Fig. 15).

It becomes obvious that it is necessary to produce deposited alloys based on more plastic phases, namely Fe_3Al and FeAl. To reduce the aluminium content in the deposited metal, double-arc surfacing using Sv-08G2S steel electrode wire and SvA7 aluminium electrode wire was proposed.

The double-arc surfacing modes were changed in the following ranges: arc voltage when using aluminium electrode wire (*U*arc Al) – from 14 to 18 V; arc voltage when using Sv-08G2S electrode wire (*U*arc St) – from 23.5 to 27.5 V; surfacing speed (*V*s) – from 0.1 to 0.2 m/min; speed of aluminium electrode wire feed (*V*f/w Al) – from 3 to 5 m/min; speed of Sv-08G2S electrode wire feed (*V*f/w St) – from 3 to 4 m/min. As the studies have shown, beads with stable geometric parameters are formed in the selected range of modes (Fig. 16).

The chemical composition of the deposited alloys varied depending on the surfacing modes within the range from 7 to 27.5 wt. % of aluminium and from 71.5 to 92 wt. % of iron, the content of impurities did not exceed 1 wt. %. The dependence of the content of aluminium and iron in the welding bead on the surfacing modes is described by regression equations:

$$\mathrm{Al} = 32.45 + 2.01 \times Vf/w\,\mathrm{Al} + 0.17 \times Vf/w\,\mathrm{Fe} + \\ + 1.64 \times V\mathrm{s} - 0.33 \times Uarc\,\mathrm{Al} - 0.83 \times Uarc\,\mathrm{Fe};$$

$$\mathrm{Fe} = 66.8 - 1.99 \times Vf/w\,\mathrm{Al} - 0.18 \times Vf/w\,\mathrm{Fe} - \\ - 1.56 \times V\mathrm{s} + 0.33 \times Uarc\,\mathrm{Al} + 0.82 \times Uarc\,\mathrm{Fe}.$$

The heterogeneity of the chemical composition across the section of the deposited metal did not exceed 3 %.

The structure of the deposited alloys is represented by the α-Fe matrix phase with partial ordering according to the B2 type, and the inclusions are the Fe_3AlC_x carbide phase (Fig. 17). The volume of inclusions in the matrix phase varies from 3.26 to 18.95 %.

The hardness of the deposited metal varies in the range from 20 to 58 HRC (Fig. 18). It is noted that with an increase in the aluminium content, the hardness increases, which is associated with an increase in the proportion of solid intermetallic phases in the coating structure.

a

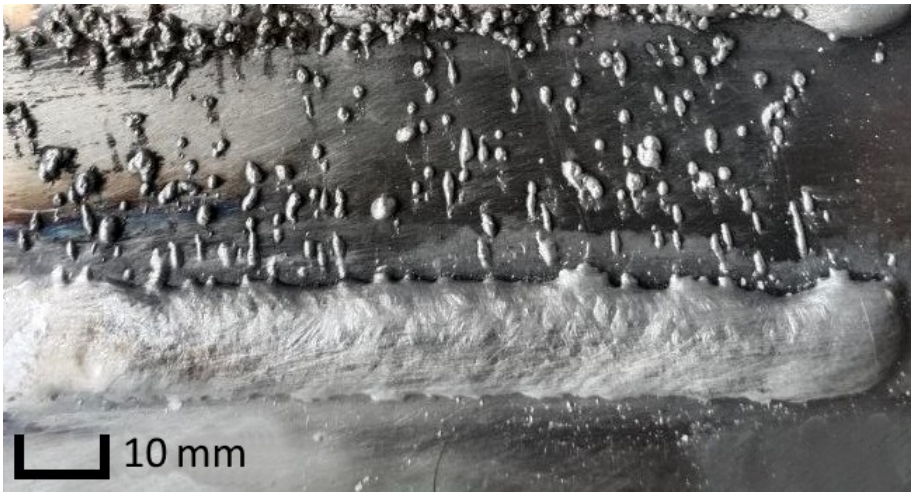

b

Fig. 10. *External appearance of the welding bead produced in the following mode: Vf/w Al=6 m/min; Uarc Al=25 V; Vs=0.15 m/min. A torch tilt angle:* ***a*** *– 90°;* ***b*** *– 30°*
Рис. 10. *Внешний вид наплавленного валика, полученного при следующем режиме: Vп/п Al=6 м/мин; Uд Al=25 В; Vн=0,15 м/мин. Угол наклона горелки:* ***a*** *– 90°;* ***b*** *– 30°*

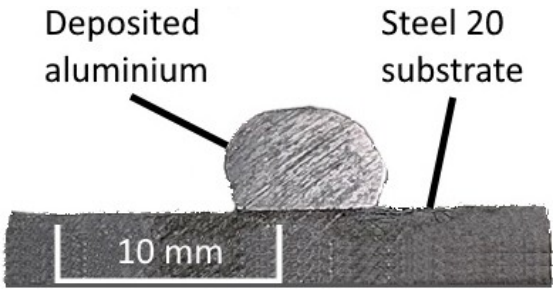

Fig. 11. *Cross-section of the deposited aluminium bead produced in the following mode: Vf/w Al=5 m/min; Uarc Al=17.5 V; Vs=0.2 m/min*
Рис. 11. *Поперечное сечение наплавленного алюминиевого валика, полученного при следующем режиме: Vп/п Al=5 м/мин; Uд Al=17,5 В; Vн=0,2 м/мин*

The relative wear resistance of the deposited metal varies in the range from 1.6 to 2.5 units. Maximum wear resistance is observed with an aluminium content of about 20 % (Fig. 19).

Heat resistance tests for 3000 h at a temperature of 950 °C showed that the deposited metal has high heat resistance. An increase in the aluminium content “refines” the surface of the welding bead; the presence of an oxide film ensures reliable protection of the metal from contact with the atmosphere. The loss of mass of the samples during heat resistance tests gradually decreases with an increase in the aluminium content from 9 to 20 %. With an aluminium content of 9–10 %,

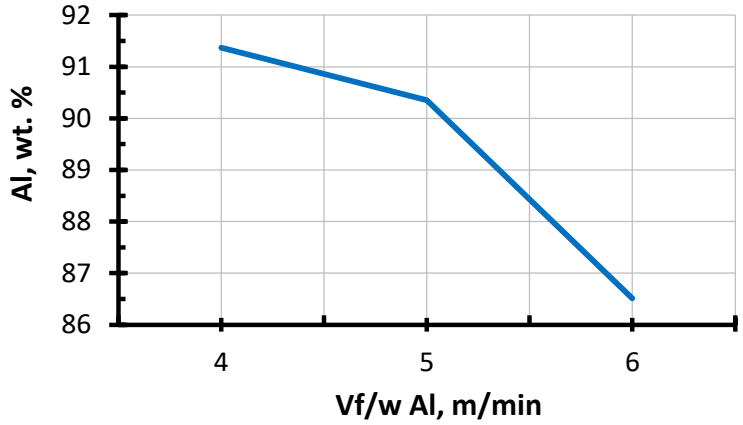

Fig. 12. *Effect of the feed rate of the aluminium electrode wire on the aluminium content in the deposited metal (Uarc Al=22.5 V; Vs=0.1 m/min)*
Рис. 12. *Влияние скорости подачи алюминиевой электродной проволоки на содержание алюминия в наплавленном металле (Uд Al=22,5 В; Vн=0,1 м/мин)*

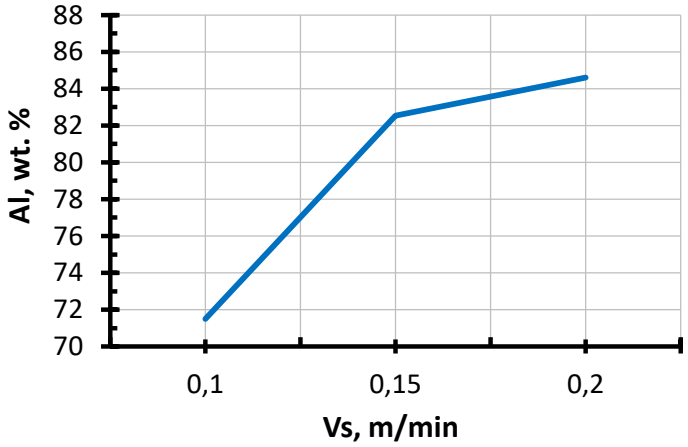

Fig. 13. *Effect of surfacing speed on the aluminium content in the deposited metal (Uarc Al=25 V; Vf/w Al=5 m/min)*
Рис. 13. *Влияние скорости наплавки на содержание алюминия в наплавленном металле (Uд Al=25 В; Vп/п Al=5 м/мин)*

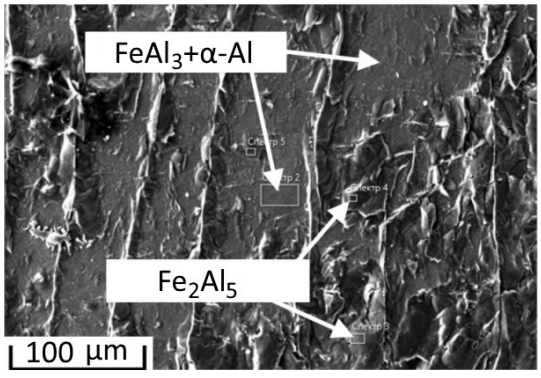

Fig. 14. *Microstructure of the deposited sample of the Fe–Al system (Vf/w Al=5 m/min; Uarc Al=20 V; Vs=0.15 m/min)*
Рис. 14. *Микроструктура наплавленного образца системы Fe–Al (Vп/п Al=5 м/мин; Uд Al=20 В; Vн=0,15 м/мин)*

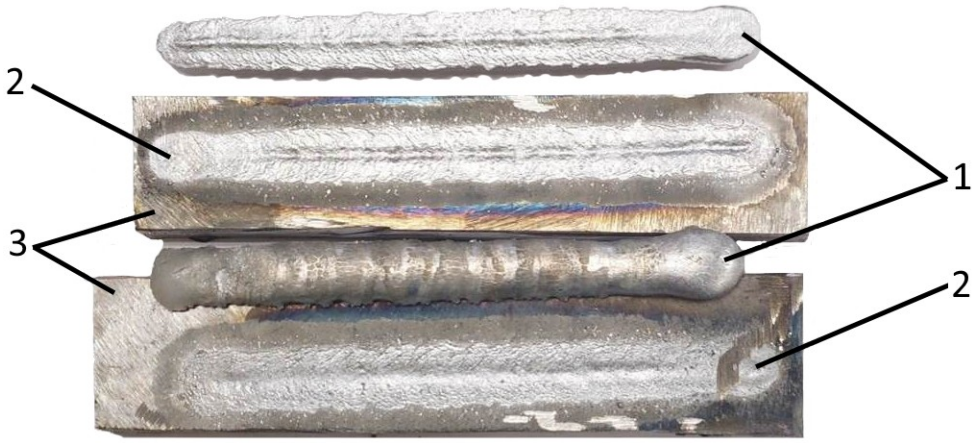

Fig. 15. *External appearance of deposited alloys peeled off from the substrates:*
1 – deposited alloys; 2 – fracture boundaries; 3 – base metal
Рис. 15. *Внешний вид наплавленных сплавов, отслоившихся от подложки:*
1 – наплавленные сплавы; 2 – граница разрушения; 3 – основной металл

Fig. 16. *External appearance of the welding bead produced by double-arc surfacing in the following mode:*
Vf/w Al=3 m/min; Vf/w Fe=3 m/min; Vs=0.15 m/min; Uarc Al=17 V; Uarc Fe=27.5 V
Рис. 16. *Внешний вид наплавленного валика, полученного двухдуговой наплавкой при следующем режиме:*
Vп/п Al=3 м/мин; Vп/п Fe=3 м/мин; Vн=0,15 м/мин; Uд Al=17 В; Uд Fe=27,5 В

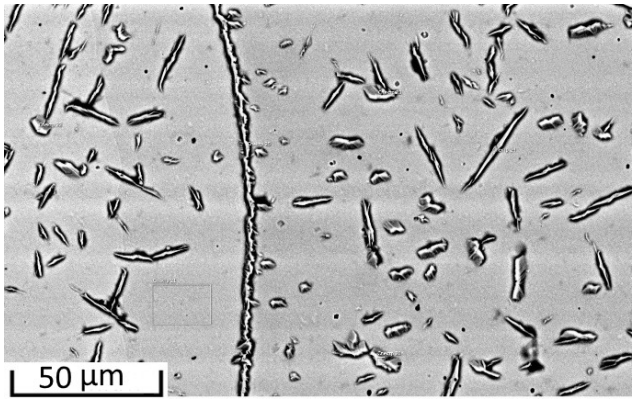

Fig. 17. *Microstructure of the deposited sample with the α-Fe matrix phase and 6 % of Fe_3AlC_x phase inclusions*
Рис. 17. *Микроструктура наплавленного образца с матричной фазой α-Fe и 6 % включений фазы Fe_3AlC_x*

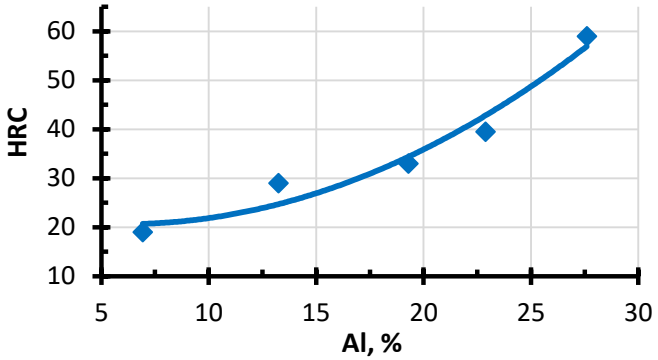

Fig. 18. *Dependence of the hardness of the deposited metal on the percentage content of aluminium*
Рис. 18. *Зависимость твердости наплавленного металла от процентного содержания алюминия*

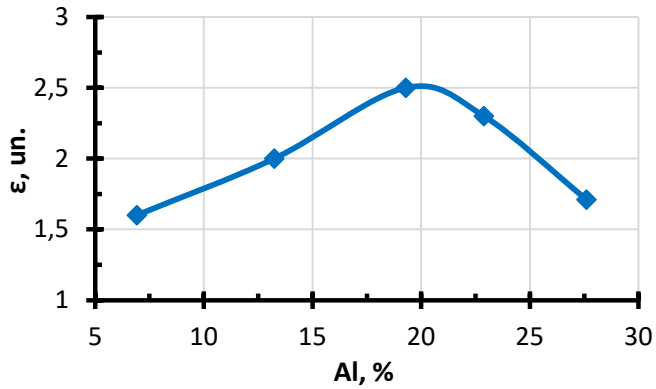

Fig. 19. *Dependence of relative wear resistance under abrasive wear on the percentage content of aluminium*
Рис. 19. *Зависимость относительной износостойкости при абразивном изнашивании от процентного содержания алюминия*

the mass loss was about 5 %, and with an aluminium content of 17–20 % – no more than 1 %. The aluminium content in the welding bead of more than 20 % leads to the appearance of a significant number of cracks and microcracks in the welding bead, which sharply reduces the heat resistance of the metal during tests. The loss of mass of samples with an aluminium content of more than 25 % during holding for 3000 h was more than 75 %. Thus, alloys containing 15 to 20 % aluminium have maximum heat resistance (Fig. 20).

DISCUSSION

The study found that single-arc surfacing of intermetallic alloys of the Fe–Al system using aluminium electrode wire does not provide a stable and predictable composition and properties of coatings based on iron aluminides. This is related to the high aluminium content in the deposited metal and the formation of alloys based on the $FeAl_3$ and α-Al phases, as well as Fe_2Al_5 and $FeAl_3$ intermetallic inclusions, which, according to observations, leads to delamination of the deposited layer from the substrate.

This phenomenon is apparently determined by the uneven distribution of intermetallic phases and the high $FeAl_3$ concentration, which contributes to the formation of microcracks and a decrease in the ductility of the deposited layer, especially along the fusion line. In [6; 7], the authors consider the properties and work for the formation of coatings based on the Fe_3Al or FeAl intermetallic phases due to their better ductility and resistance to cracking at room temperature. In this regard, for producing wear-resistant and durable coatings on steel parts, methods that allow forming coatings with a chemical and phase composition based on the Fe_3Al and FeAl phases are more promising. However, the known methods of applying protective coatings based on iron aluminides allow producing coatings with a limited layer thickness of up to 0.5 mm, which is clearly insufficient for mining equipment components operating under abrasive wear conditions. Another significant limitation of existing

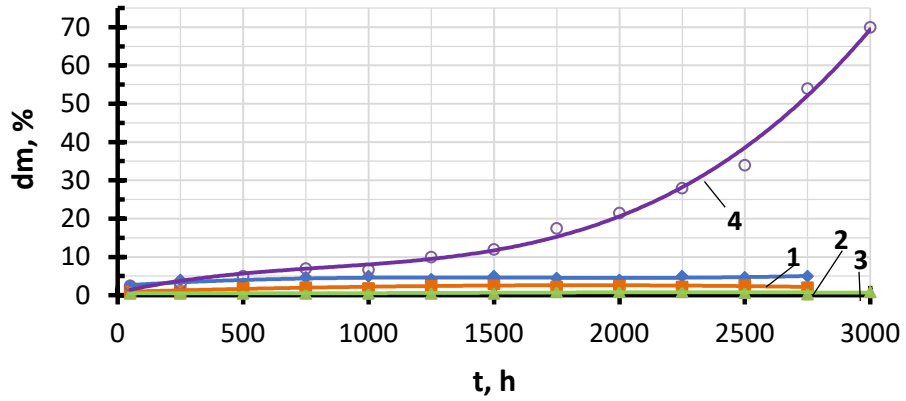

Fig. 20. *Dependence of the change in the mass of samples on the time of their holding at a temperature of 950 °C with an aluminium content of:*
1 – 7 %; 2 – 14 %; 3 – 17 %; 4 – 25 %
Рис. 20. *Зависимость изменения массы образцов от времени их выдержки при температуре 950 °С с содержанием алюминия: 1 – 7 %; 2 – 14 %; 3 – 17 %; 4 – 25 %*

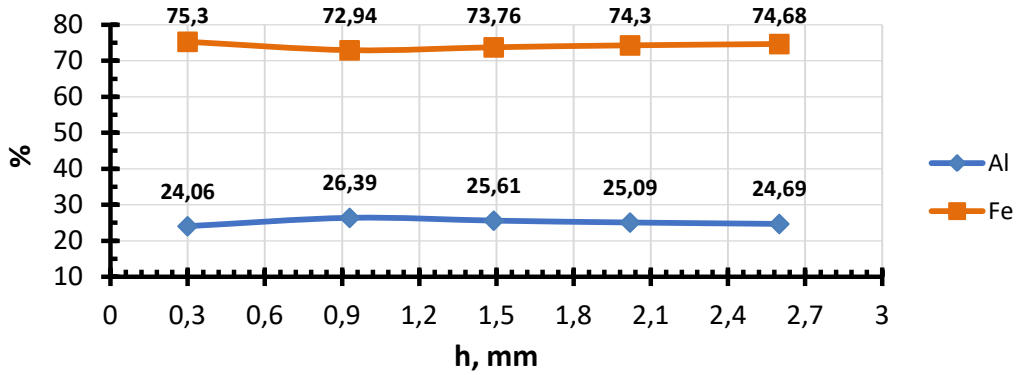

Fig. 21. *Graph of the percentage content of aluminium and iron in the cross-section of the deposited metal (Uarc Al=14 V; Vf/w Al=5 m/min; Uarc Fe=23.5 V; Vf/w Fe=3 m/min; Vs=0.1 m/min)*
Рис. 21. *График процентного содержания алюминия и железа по сечению наплавленного металла (Uд Al=14 В; Vп/п Al=5 м/мин; Uд Fe=23,5 В; Vп/п Fe=3 м/мин; Vн=0,1 м/мин)*

methods is the impossibility of applying coatings under installation conditions and the lack of prospects for further restoration of the coating after wear.

Therefore, for mining parts operating in tough environment, it is necessary to apply methods that combine the possibilities of producing coatings with a phase composition based on Fe_3Al or FeAl, as well as the possibility of producing coatings thicker than 0.5 mm. Such methods may include automatic argon-arc surfacing with a noncomsumable electrode [19] or double-arc surfacing using steel and aluminium electrode wires. In particular, the double-arc technology allows achieving better homogeneity of the chemical composition (Fig. 21).

A study of the effect of double-arc surfacing modes showed that changing the wire feed speed, voltage and torch angle significantly affects the properties of the resulting layers. In particular, an increase in the aluminium content to 27 wt. % contributes to an increase in the hardness of the deposited alloys to 58 HRC. However, this is accompanied by a decrease in ductility and an increase in the risk of cracking.

Wear tests showed that maximum wear resistance is achieved with an aluminium content of about 20 %, which is associated with an optimal ratio of hardness and microstructural stability. These results coincide with the data of [10; 11], where it is noted that the content of intermetallic phases and their distribution significantly affect the wear resistance of coatings. At the same time, there is no direct correlation between hardness and wear resistance, which indicates the importance of microstructural factors such as the size and distribution of intermetallic inclusions.

As for heat resistance, the results show that the aluminium content in the range of 15–20 % provides the maximum resistance to high temperatures. This is due to the formation of an oxide film, which serves as a protective barrier and prevents metal oxidation. However, an increase in the aluminium content above 20 % leads to the appearance of microcracks and a decrease in heat resistance, which is

consistent with the data of [14; 16; 17], where it is noted that excess aluminium contributes to the formation of internal stresses and defects.

The obtained results allow recommending double-arc surfacing as a method for applying wear-resistant coatings based on iron aluminides for low-carbon steel parts used in the mining industry or as a substitute for expensive coatings, since it allows producing coatings with a thickness of up to 5 mm. The discovered patterns allow concluding that the optimal composition for wear-resistant and heat-resistant coatings of the Fe–Al system is in the range of 15–20 % of aluminium. An important direction for further research is the development of methods for monitoring and stabilising the microstructure, as well as studying the effect of additional alloying elements on the properties of coatings. Moreover, it is necessary to study in more detail the mechanisms of formation of intermetallic phases and their influence on the adhesion and durability of coatings.

A limitation of this study is the limited range of modes and the lack of long-term tests under operating conditions. In the future, it is planned to expand the range of modes, as well as conduct wear and heat resistance tests under real operating loads.

CONCLUSIONS

1. Double-arc surfacing allows creating wear-resistant coatings of the Fe–Al system on low-carbon steel products used under conditions of abrasive wear and high temperatures reaching 950 °C.

2. By controlling the parameters of the double-arc surfacing process, it is possible to create deposited layers of intermetallic alloys with specified properties adapted to specific operating conditions due to the variation of their chemical and phase composition.

3. The chemical composition of the deposited alloys is characterised by an aluminium content in the range from 7 to 27.5 wt. %. The basis of the structure is the α-Fe matrix partially ordered according to the B2 type, and the inclusions present are the Fe_3AlC_x carbide phase. The volume of carbide inclusions varies from 3.26 to 18.95 %.

4. Fe–Al system alloys produced by double-arc surfacing have high hardness (20–58 HRC), wear resistance and heat resistance.

REFERENCES

1. Grechneva M.V., Tolkachev S.A., Vladimirtsev I.K. Increasing wear resistance of mining machinery parts. *Proceedings of Irkutsk State Technical University,* 2011, no. 12, pp. 26–29. EDN: ONXUEZ.
2. Isagulov A.Z., Kvon S.S., Kulikov V.Yu. Improving wear resistance of elements of mining and processing equipment. *Ferrous Metallurgy. Bulletin of Scientific, Technical and Economic Information*, 2020, vol. 76, no. 6, pp. 609–613. DOI: 10.32339/0135-5910-2020-6-609-613.
3. Nikitenko M.S., Knyazkov K.V., Ababkov N.V., Ozhiganov E.A. Development of diagnostic, restoration and strengthening complex for mining equipment. *Mining Informational and Analytical Bulletin*, 2013, no. S6, pp. 447–456. EDN: RYYJAP.
4. Korotkova V.A., Zamotina V.A. Restoration of mining equipment components. *Gornyi zhurnal*, 2001, no. 8, pp. 53–58.
5. Ivanov A.V., Priozerskaya O.L. Promising methods of welding deposition and machining of parts restored. *Technico-tehnologicheskie problemy servisa*, 2010, no. 3, pp. 7–9. EDN: MVHIZL.
6. Palm M., Stein F., Dehm G. Iron aluminides. *Annual Review of Materials Research*, 2019, vol. 49, pp. 297–326. DOI: 10.1146/annurev-matsci-070218-125911.
7. Moszner F., Peng J., Suutala J., Jasnau U., Damayi M., Palm M. Application of iron aluminides in the combustion chamber of large bore 2-stroke marine engines. *Metals*, 2019, vol. 9, no. 8, article number 847. DOI: 10.3390/met9080847.
8. Kumar A., Nayak S.K., Laha T. Comparative Study on Wear and Corrosion Behavior of Plasma Sprayed $Fe_{73}Cr_2Si_{11}B_{11}C_3$ and $Fe_{63}Cr_9P_5B_{16}C_7$ Metallic Glass Composite Coatings. *Journal of Thermal Spray Technology*, 2022, vol. 31, pp. 1302–1316. DOI: 10.1007/s11666-021-01280-1.
9. Metidji N., Younes A., Allou D., Dilmi N. Effect of zirconium of the corrosion behavior of $FeAl_{40}Ti_3B$ intermetallic compounds for use in solar water heaters. *Journal of Applied Electrochemistry*, 2024, vol. 54, pp. 1267–1277. DOI: 10.1007/s10800-023-02033-4.
10. Ravi K., Batra U., Prakash U. Investigation of mechanical and wear characteristics of forged Fe-Al-C intermetallic quaternary alloyed with Zr/Ti. *Journal of Materials Engineering and Performance*, 2022, vol. 31, pp. 3127–3135. DOI: 10.1007/s11665-021-06424-6.
11. Metidji N., Younes A. Effects of boron, nickel and molybdenum content on the microstructure, mechanical behaviour and wear properties of FeAl alloy made by vacuum arc melting. *Transactions of the Indian Institute of Metals*, 2022, vol. 75, pp. 2691–2699. DOI: 10.1007/s12666-022-02639-w.
12. De Sousa Malafaia A.M., Maestro C.A.R., de Oliveira M.F. Alternative air induction melt–remelt processing of an Fe3Al–C intermetallic alloy: part I – mechanical properties and the effects of loading rate, heat treatment and test temperatures. *International Journal of Metalcasting*, 2022, vol. 16, pp. 1265–1275. DOI: 10.1007/s40962-021-00679-4.
13. De Sousa Malafaia A.M., Maestro C.A.R., de Oliveira M.F. Alternative air induction melt–remelt processing of an Fe_3Al–C intermetallic alloy: part II – high temperature cyclic oxidation behavior. *International Journal of Metalcasting*, 2023, vol. 17, pp. 1673–1680. DOI: 10.1007/s40962-022-00881-y.
14. Deevi S.C. Advanced intermetallic iron aluminide coatings for high temperature applications. *Progress in Materials Science*, 2021, vol. 118, article number 100769. DOI: 10.1016/j.pmatsci.2020.100769.
15. Martins N., Silva A.P., Cordeiro Da Silva G., Dos Dantos I.B., Santos C.E.D., Troysi F., Brito P. Characterization of Iron Aluminide Diffusion Coatings Obtained after Friction Surfacing. *Metals*, 2023, vol. 13, article number 461. DOI: 10.3390/met13030461.

16. Troysi F.D., Brito P.P. Development and characterization of an iron aluminide coating on mild steel substrate obtained by friction surfacing and heat treatment. The *International journal of Advanced Manufacturing Technology*, 2020, vol. 111, no. 9, pp. 2569–2576. DOI: 10.1007/s00170-020-06310-w.
17. Mohammadkhani S., Bondar N., Vahdati-Khaki J., Haddad-Sabzevar M. Fabrication of Iron Aluminide Coatings (Fe_3Al and $FeAl_3$) on Steel Substrate by Self-Propagating High Temperature Synthesis (SHS) Process. *Journal of Coating Science and Technology*, 2017, vol. 4, no. 2, pp. 40–44. DOI: 10.6000/2369-3355.2017.04.02.2.
18. Chen Maolong, Yang Xuefeng, Zhang Zhiqiang, Gu Yanguang, Li Kunjie, Liu Yansheng, Ma Junbei. Research status of laser cladding technology on aluminum alloy surface. *The International journal of Advanced Manufacturing Technology*, 2025, vol. 137, no. 1-2. pp. 1–21. DOI: 10.1007/s00170-025-15204-8.
19. Kovtunov A.I., Bochkarev A.G., Plakhotnyy D.I. Study of the processes of formation of deposited alloys of the Fe-Al system alloyed with Si. *Svarochnoe proizvodstvo*, 2017, no. 12, pp. 3–7. EDN: YRIBHU.

СПИСОК ЛИТЕРАТУРЫ

1. Гречнева М.В., Толкачев С.А., Владимирцев И.К. Повышение износостойкости деталей горных машин // Вестник Иркутского государственного технического университета. 2011. № 12. С. 26–29. EDN: ONXUEZ.
2. Исагулов А.З., Квон С.С., Куликов В.Ю. Повышение износостойкости элементов горно-обогатительного оборудования // Черная металлургия. Бюллетень научно-технической и экономической информации. 2020. Т. 76. № 6. С. 609–613. DOI: 10.32339/0135-5910-2020-6-609-613.
3. Никитенко М.С., Князьков К.В., Абабков Н.В., Ожиганов Е.А. Разработка комплекса средств технической диагностики, восстановления и упрочнения элементов горнодобывающего оборудования // Горный информационно-аналитический бюллетень (научно-технический журнал). 2013. № S6. С. 447–456. EDN: RYYJAP.
4. Короткова В.А., Замотина В.А. Восстановление деталей горного оборудования // Горный журнал. 2001. № 8. С. 53–58.
5. Иванов А.В., Приозерская О.Л. Перспективные способы наплавки и механической обработки восстанавливаемых деталей // Технико-технологические проблемы сервиса. 2010. № 3. С. 7–9. EDN: MVHIZL.
6. Palm M., Stein F., Dehm G. Iron aluminides // Annual Review of Materials Research. 2019. Vol. 49. P. 297–326. DOI: 10.1146/annurev-matsci-070218-125911.
7. Moszner F., Peng J., Suutala J., Jasnau U., Damayi M., Palm M. Application of iron aluminides in the combustion chamber of large bore 2-stroke marine engines // Metals. 2019. Vol. 9. № 8. Article number 847. DOI: 10.3390/met9080847.
8. Kumar A., Nayak S.K., Laha T. Comparative Study on Wear and Corrosion Behavior of Plasma Sprayed $Fe_{73}Cr_2Si_{11}B_{11}C_3$ and $Fe_{63}Cr_9P_5B_{16}C_7$ Metallic Glass Composite Coatings // Journal of Thermal Spray Technology. 2022. Vol. 31. P. 1302–1316. DOI: 10.1007/s11666-021-01280-1.
9. Metidji N., Younes A., Allou D., Dilmi N. Effect of zirconium of the corrosion behavior of $FeAl_{40}Ti_3B$ intermetallic compounds for use in solar water heaters // Journal of Applied Electrochemistry. 2024. Vol. 54. P. 1267–1277. DOI: 10.1007/s10800-023-02033-4.
10. Ravi K., Batra U., Prakash U. Investigation of mechanical and wear characteristics of forged Fe-Al-C intermetallic quaternary alloyed with Zr/Ti // Journal of Materials Engineering and Performance. 2022. Vol. 31. P. 3127–3135. DOI: 10.1007/s11665-021-06424-6.
11. Metidji N., Younes A. Effects of boron, nickel and molybdenum content on the microstructure, mechanical behaviour and wear properties of FeAl alloy made by vacuum arc melting // Transactions of the Indian Institute of Metals. 2022. Vol. 75. P. 2691–2699. DOI: 10.1007/s12666-022-02639-w.
12. De Sousa Malafaia A.M., Maestro C.A.R., de Oliveira M.F. Alternative air induction melt–remelt processing of an Fe_3Al–C intermetallic alloy: part I – mechanical properties and the effects of loading rate, heat treatment and test temperatures // International Journal of Metalcasting. 2022. Vol. 16. P. 1265–1275. DOI: 10.1007/s40962-021-00679-4.
13. De Sousa Malafaia A.M., Maestro C.A.R., de Oliveira M.F. Alternative air induction melt–remelt processing of an Fe_3Al–C intermetallic alloy: part II – high temperature cyclic oxidation behavior // International Journal of Metalcasting. 2023. Vol. 17. P. 1673–1680. DOI: 10.1007/s40962-022-00881-y.
14. Deevi S.C. Advanced intermetallic iron aluminide coatings for high temperature applications // Progress in Materials Science. 2021. Vol. 118. Article number 100769. DOI: 10.1016/j.pmatsci.2020.100769.
15. Martins N., Silva A.P., Cordeiro Da Silva G., Dos Dantos I.B., Santos C.E.D., Troysi F., Brito P. Characterization of Iron Aluminide Diffusion Coatings Obtained after Friction Surfacing // Metals. 2023. Vol. 13. Article number 461. DOI: 10.3390/met13030461.
16. Troysi F.D., Brito P.P. Development and characterization of an iron aluminide coating on mild steel substrate obtained by friction surfacing and heat treatment // The International journal of Advanced Manufacturing Technology. 2020. Vol. 111. № 9. P. 2569–2576. DOI: 10.1007/s00170-020-06310-w.
17. Mohammadkhani S., Bondar N., Vahdati-Khaki J., Haddad-Sabzevar M. Fabrication of Iron Aluminide Coatings (Fe_3Al and $FeAl_3$) on Steel Substrate by Self-Propagating High Temperature Synthesis (SHS) Process // Journal of Coating Science and Technology. 2017. Vol. 4. № 2. P. 40–44. DOI: 10.6000/2369-3355.2017.04.02.2.
18. Chen Maolong, Yang Xuefeng, Zhang Zhiqiang, Gu Yanguang, Li Kunjie, Liu Yansheng, Ma Junbei. Research status of laser cladding technology on aluminum alloy surface // The International journal of Advanced Manufacturing Technology. 2025. Vol. 137. № 1-2. P. 1–21. DOI: 10.1007/s00170-025-15204-8.
19. Ковтунов А.И., Бочкарев А.Г., Плахотный Д.И. Исследование процессов формирования наплавленных сплавов системы Fe-Al легированных Si // Сварочное производство. 2017. № 12. С. 3–7. EDN: YRIBHU.

УДК 621.791.927.5
doi: 10.18323/2782-4039-2025-3-73-1

Особенности дуговой наплавки интерметаллидных сплавов системы Fe–Al на поверхности низкоуглеродистых сталей

Бочкарев Александр Геннадьевич*[1,3], кандидат технических наук,
доцент кафедры «Сварка, обработка материалов давлением и родственные процессы»
Ковтунов Александр Иванович[1,4], доктор технических наук,
профессор кафедры «Сварка, обработка материалов давлением и родственные процессы»
Плахотный Денис Иванович[1,5], старший преподаватель
кафедры «Сварка, обработка материалов давлением и родственные процессы»
Хохлов Юрий Юрьевич[1,6], заведующий лабораторией
кафедры «Сварка, обработка материалов давлением и родственные процессы»
Белоногов Савелий Олегович[2,7], инженер лаборатории разрушающих методов контроля
Веденеев Иван Вячеславович[2,8], инженер лаборатории неразрушающего контроля
[1]*Тольяттинский государственный университет, Тольятти (Россия)*
[2]*ООО «Средневолжский сертификационно-диагностический центр «Дельта», Тольятти (Россия)*

***E-mail:** a.bochkarev5@tltsu.ru,
a.bochkarev93@mail.ru

[3]ORCID: https://orcid.org/0000-0002-7945-1634
[4]ORCID: https://orcid.org/0000-0002-7705-7377
[5]ORCID: https://orcid.org/0000-0003-2021-8974
[6]ORCID: https://orcid.org/0000-0002-5276-8957
[7]ORCID: https://orcid.org/0009-0007-9788-9967
[8]ORCID: https://orcid.org/0009-0009-4159-526X

Поступила в редакцию 17.04.2025 *Пересмотрена 10.06.2025* *Принята к публикации 13.08.2025*

Аннотация: Долговечность деталей, используемых в промышленности, во многом определяется материалами, из которых они изготовлены. Зачастую применяемые материалы должны быть устойчивыми к износу, коррозии и высоким температурам. Современные материалы, такие как высокопрочные легированные стали, обладают высокой стоимостью и ограниченной свариваемостью, что усложняет восстановление изношенных деталей. В качестве альтернативы рассматриваются сплавы системы Fe–Al, обладающие высокой коррозионной стойкостью, износостойкостью и жаростойкостью при меньшей стоимости. Цель исследования – повышение износостойкости и жаростойкости деталей из низкоуглеродистой стали путем исследования процессов дуговой наплавки алюминидов железа и их свойств. Методика исследования включала однодуговую и двухдуговую наплавку с использованием алюминиевой и стальной электродных проволок, анализ химического состава наплавленных покрытий, их твердости, износостойкости и жаростойкости. Результаты показали, что однодуговая наплавка формирует сплавы на основе фаз $FeAl_3$ и α-Al с включениями Fe_2Al_5 и $FeAl_3$, а двухдуговая – более насыщенные железом сплавы с матричной фазой α-Fe и карбидной фазой Fe_3AlC_x. Полученные сплавы демонстрируют твердость до 58 HRC, относительную износостойкость до 2,5 ед. и потерю массы не более 5 % при содержании алюминия до 20 %, что говорит об их перспективности для применения в условиях повышенных нагрузок. Результаты подтверждают целесообразность использования алюминидов железа как недорогой альтернативы дорогостоящим покрытиям, что расширяет возможности повышения износостойкости и жаростойкости деталей в промышленности.

Ключевые слова: дуговая наплавка; интерметаллидные сплавы; алюминиды железа; низкоуглеродистая сталь; твердость; износостойкость; жаростойкость.

Для цитирования: Бочкарев А.Г., Ковтунов А.И., Плахотный Д.И., Хохлов Ю.Ю., Белоногов С.О., Веденеев И.В. Особенности дуговой наплавки интерметаллидных сплавов системы Fe–Al на поверхности низкоуглеродистых сталей // Frontier Materials & Technologies. 2025. № 3. С. 11–25. DOI: 10.18323/2782-4039-2025-3-73-1.